Long-range influence of steps on water adsorption on clean and D-covered Pt surfaces

Dunnen, A. den; Niet, M.J.T.C. van der; Badan, C.; Koper, M.T.M.; Juurlink, L.B.F.

PCCP

PAPER

View Article Online
View Journal | View Issue

Cite this: *Phys. Chem. Chem. Phys.*, 2015, **17**, 8530

Long-range influence of steps on water adsorption on clean and D-covered Pt surfaces

Angela den Dunnen, Maria J. T. C. van der Niet, Cansin Badan, Marc T. M. Koper and Ludo B. F. Juurlink*

Received 17th July 2014,
Accepted 22nd September 2014

DOI: 10.1039/c4cp03165b

www.rsc.org/pccp

We have examined water desorption from Pt(111) terraces of varying width and its dependence on precoverage by deuterium (D) with temperature programmed desorption studies. We observe distinct water desorption from (100) steps and (111) terraces, with steps providing adsorption sites with a higher binding energy than terraces. Preadsorption of D at the steps causes annihilation of water stabilization at the steps, while it also causes an initial stabilization of water on the (111) terraces. When the (111) terraces also become precovered with D, this water stabilization trend reverses on all surfaces. Destabilization continues for stepped surfaces containing up to 8-atom wide (111) terraces with a (100) step type and these become hydrophobic, in contrast to surfaces with a (110) step type and with the infinite (111) terrace. Our results illustrate how surface defects and a delicate balance between intermolecular forces and the adsorption energy govern hydrophobic *vs.* hydrophilic behavior, and that the influence of steps on the adsorption of water on nano-structured platinum surfaces has a very long-ranged character.

1 Introduction

The structure of water at interfaces and the associated hydrophilicity and hydrophobicity are important in fields such as biology, astrophysics, chemistry, and physics.[1–13] In biology, one could think of the folding of proteins,[2,3] or micelles,[4,5] where hydrophilic and hydrophobic interactions play an important role. Water structures are also found in space, *e.g.* on interstellar dust grains and comets. These water structures play an important role in the formation of planets and stars.[6–8] In the field of materials and surface science, self-assembled monolayers are studied to design functional surfaces. The characteristics of such surfaces can be fine tuned from very hydrophilic to very hydrophobic by using different functional groups.[9,10] Single-walled carbon nanotubes are used as model systems to study interfacial properties of nanoconfined water. Water can form a hydrogen-bonded network through the hydrophobic tubes.[11,12] A change in temperature can result in a hydrophobic–hydrophilic transition.[13] The interaction between water and metal catalysts is also important in electrochemical systems such as low temperature fuel cells and other aqueous electrochemical systems. In these systems, water and other molecules interact with a metallic electrode material.

Three extensive reviews have summarized the interaction and reaction of water and co-adsorbates with metal and metal oxide surfaces.[14–16] These studies show that the interfacial water structure depends, amongst other variables, on the metal identity and atomic structure, the surface temperature, and pressure. On surfaces such as Cu(111), Ag(111), and Au(111), water forms 3-D ice clusters, implying that these surfaces are non-wetting. On other surfaces, such as Pt(111), Pd(111), and Ru(0001), water initially forms a wetting layer. The structure of this first layer determines whether or not a second wetting layer is formed.[16] Even the unit cell structure of the first layer varies with metal identity and atomic structure. On Pt(111), a hexagonal water structure is formed,[17] whereas on Cu(110) interlinked pentamers have been observed.[18] It is also well documented that depending on the growth temperature, various multilayered structures can be formed. A water monolayer dosed on a Pt(111) surface at temperatures below 135 K, yields so-called amorphous solid water (ASW).[19] When water is dosed at a higher temperature, or during a temperature ramp, crystalline ice (CI) structures are formed.[17]

Single atomic steps at surfaces may also influence the structure of adsorbed water. Thürmer and Nie showed that cubic ice (I_c) is grown in spirals created by screw dislocations above substrate steps.[20] They also showed that in thin water films, hexagonal ice (I_h) is favored, while in thicker films, mostly I_c is formed. In the submonolayer regime, Morgenstern *et al.* showed, using scanning tunneling microscopy (STM), that water adsorbs preferentially at the upper side of steps at low coordination sites on Pt(111). For rectangular (110) steps, short chains or clusters seemed to appear, whereas for the square

Leiden Institute of Chemistry, Leiden University, Einsteinweg 55, P.O. Box 9502, 2300 RA Leiden, The Netherlands. E-mail: l.juurlink@chem.leidenuniv.nl; Tel: +31 (0)71 527 4221

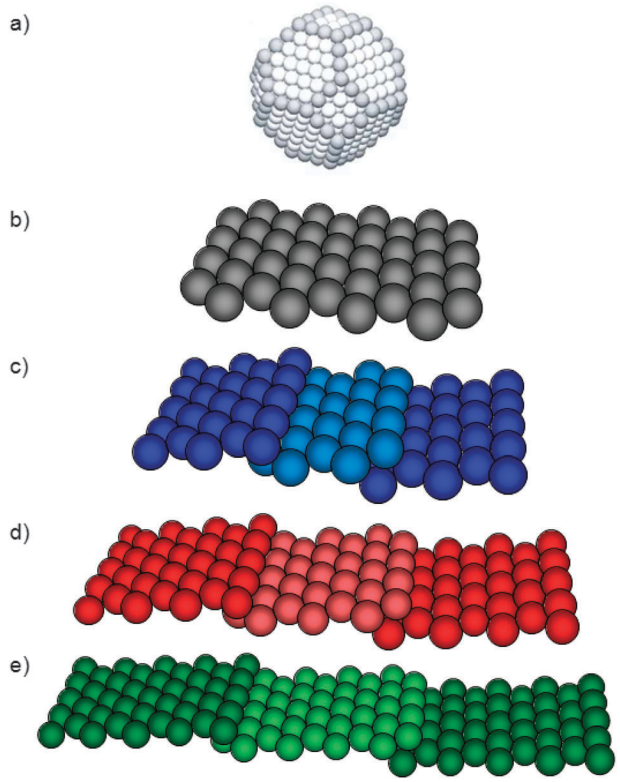

Fig. 1 Schematic representation of (a) 2.74 nm diameter Pt nanoparticle, from,[24] (b) Pt(111), (c) Pt(533), (d) Pt(755), and (e) Pt(977).

(100) steps, molecular chains are formed.[21] On Ag(111), a 1-D amorphous structure is formed when water is adsorbed at 70 K. A 2-D bilayer grows at the lower step edge, on which a second layer nucleates heterogeneously.[22]

The steps and defects in the (111) facet are believed to be catalytically active sites for many reactions.[23] Water prefers to bind at step edges and corners on catalyst nanoparticles (grey atoms in Fig. 1a). This figure shows a schematic representation of an fcc metal catalyst particle with square (100) and hexagonal (111) facets.[24] The terrace length and amount of defects depend on the diameter of the nanoparticle. The presence of the various surface structures makes it difficult to study fundamental reaction steps on nanoparticles. To gain more insight in the catalytic activity at platinum surfaces, Pt single crystals have been studied. The (111) facet is modeled by a Pt(111) surface (Fig. 1b). The effect of defect sites can be modeled by the use of stepped single crystal surfaces, *e.g.* using variable terrace lengths (Fig. 1c–e).

Platinum is a good catalyst for many electrochemical reactions, where the interaction of water with the Pt surface as well as with other species is relevant. The interaction of water with Pt(111) is well studied and shows considerable complexity.[17,19,21,25–36] Fewer experimental studies have investigated the interaction of water with platinum surfaces with defects that are naturally present on the surface,[21] or regularly stepped surfaces.[37–39] In systems such as the hydrogen–oxygen fuel cell other species, *e.g.* adsorbed hydrogen or oxygen atoms and hydroxyl groups, are also present. Therefore, co-adsorption studies including water at different platinum surfaces are highly relevant and may serve as model systems. D_2O on a Pt(111) surface is slightly stabilized in the presence of a small amount of deuterium.[40] For higher D-precoverage, it is approximately as stable as on the bare Pt(111) surface. Both bare Pt(111) and D/Pt(111) are hydrophilic, *i.e.* water wets the surface prior to forming multilayered structures. We have shown previously that pre-deuteration of surfaces with (100) and (110) steps separating short 4-atom wide (111) terraces has very different effects, depending on the step geometry. On both surfaces, the step-related stabilization of water disappears when a small amount of D is precovering the surfaces. The pre-deuterated surface with (110) steps is still hydrophilic. Conversely, the pre-deuterated surface with (100) steps is hydrophobic. Water forms ASW clusters near step sites on D/Pt(533).[41]

Here, we expand upon our elucidation of the water structures in contact with bare and pre-deuterated stepped Pt surfaces with (100) steps and (111) terraces (Pt[n(111) × (100)]). The terrace width (n) varies form 4 (Pt(533), Fig. 1c), to 6 (Pt(755), Fig. 1d), to 8 atoms (Pt(977), Fig. 1e). This reflects relevant nanoparticle systems with a diameter up to ~7 nm. We compare the results of the stepped surfaces to the flat Pt(111) surface. We use temperature programmed desorption (TPD) in combination with isotopic labeling, to investigate the role of terrace width in the hydrophobicity/hydrophilicity and the exchange between D_{ad} and H_2O. Significantly, our results show a strongly long-range influence of step sites on the adsorption of water layers on clean and D-covered platinum surfaces, showing that the perturbative effect that defects may have on water-covered Pt surfaces extends well beyond the immediate vicinity of the defect.

2 Experimental

Experiments were performed in an ultra-high vacuum (UHV) apparatus containing LEED/Auger Electron Spectroscopy (LK Technologies, RVL 2000/8/R), a quadrupole mass spectrometer (QMS, Pfeiffer QME 200), and various leak valves. The base pressure of the system was 2×10^{-10} mbar during experiments. The Pt crystals (cut and polished $<0.1^{\circ}$, Surface Preparation Laboratory, Zaandam, The Netherlands) were cleaned by repeated cycles of Ar^+ bombardment (Messer, 5.0; 20 μA, 10 min), annealing between 850 and 1000 K in an oxygen atmosphere (Messer, 5.0; 2×10^{-8} mbar), and annealing at 1200 K. The crystal temperature can be controlled between 84 and 1200 K with the use of liquid nitrogen for cooling and radiative heating combined with electron bombardment for heating.

Water from a Millipore Milli-Q gradient A10 system (18.2 MΩ resistance) was deaerated in a glass container by multiple freeze–pump–thaw cycles and kept at a total pressure of 2.0 bar helium (Air Products, BIP Plus). A water bath (~30 °C) was used to keep the vapor pressure of the water in the glass container constant. The container was connected to a home-built glass capillary-array doser located ~1.5 cm from the sample. Water was dosed directly on the surface at $T_s \leq 110$ K

at a rate of ~ 0.009 ML s^{-1} by measuring the pressure rise due to the co-dosed helium.

To minimize hydrogen contamination from background adsorption, all filaments were switched off during D_2 dosing (Lindegas, 2.8; background dosing, 2×10^{-7} mbar while cooling down the sample from 500 to 100 K (~ 5 min)). This produced a full monolayer of D_{ad}. To vary the amount of deuterium on the surface, we first create a full monolayer of D_{ad}, then we remove a part from the surface by ramping the crystal to a set temperature with 1 K s^{-1} and subsequently cooling the crystal to 100 K before measuring TPD spectrum. All reported pressures are uncorrected for ion gauge sensitivity.

For the co-adsorption experiments, deuterium was adsorbed first. After the pressure in the system had reached the base pressure, water was dosed on top of the (partly) deuterated surface.

For TPD spectroscopy the heating rate was 1 K s^{-1}. During heating m/z = 2 (H_2), 3 (HD), 4 (D_2), 18 (H_2O), 19 (HOD), and 20 (D_2O) were monitored with the QMS. We have verified that cracking in the QMS ionizer of HOD and D_2O yields no significant contribution to the signal at m/z = 18 at the low signal intensities in experiments for m/z = 19 and 20. Therefore, the signal at m/z = 18 results only from H_2O within experimental error. Similarly, the signal at m/z = 19 results only from HOD and the signal at m/z = 20 only from D_2O. Experiments where only water is dosed onto the crystal show that there is no significant amount of m/z = 20 desorbing from the surface (either from $H_2{}^{18}O$ or D_2O). Therefore, we do believe that in our experiments with co-adsorption of D_2 and H_2O, m/z = 20 results from D_2O desorption and not from $H_2{}^{18}O$. For data analysis m/z = 2 was not taken into account, since the signal is negligibly small and mainly due to D^+ and not $H_2{}^+$. Initially, m/z = 28 (CO) and 32 (O_2) were monitored as well, but no desorption was detected. All H_2O and D_2 coverages are calculated from the integrated TPD peak areas. Following Grecea *et al.*,[38] we define 1 monolayer (ML) of water as the largest combined integral for the two high temperature peaks on each of the stepped Pt surfaces, or the integral of the single high temperature peak for Pt(111). We are not aware of an unambiguous means to determine the integral for 1 ML HOD desorbing from the surface. Therefore, we have used the integral for 1 ML H_2O (desorbing from bare Pt) as a reference in quantifying the amounts of H_2O and HOD. We assume that the cracking ratio in the QMS and channeltron amplification are similar for both isotopes, because of the relatively small difference in mass/charge ratio. We define 1 ML of deuterium as the maximum integrated area of the spectrum, without implying a D_{ad} : Pt ratio of 1 : 1, as was shown for the Pt(533) surface.[39] We have corrected the temperature of the Pt(755), Pt(977), and Pt(111) surfaces by shifting the complete temperature range by at most 3.3 K. We have done this in order to align the onset of the second water layer desorption to that of Pt(533). This may be expected to be the same for every crystal independent of its structure or type of metal,[16] although we acknowledge that kinetic factors may play a role leading to differences between the various step widths. Here, we expect that small changes in the temperature readout of the different crystals are caused by differences in the attachment of the thermocouple wires to the various crystals. We therefore believe that the temperature shift is reasonable and necessary.

The H_2O TPD spectra show an almost stepwise increase in their baseline. This is due to the high vacuum time constant of water in our UHV system. A reasonable approximation for the baseline is given by:

$$y = y_0 + \frac{1}{2}\Delta y \times \left(\tanh\left(\frac{T - T_0}{\Delta T}\right) + 1\right) \quad (1)$$

where Δy is the total increase in the height of the baseline, T_0 is the center of the *S*-curve, typically slightly before the peak maximum, and ΔT is an arbitrary parameter to smooth out the tanh. Note that the value of ΔT does not matter for the total obtained integral, though it may affect the relative intensities of smaller peaks at lower temperatures. We have verified that this baseline correction procedure does not influence the leading edges of our TPD data if ΔT and T_0 are kept constant. An example of the raw data and the background correction of water desorption from Pt(553) was shown in a previous article.[42]

3 Results and discussion

3.1 H_2O desorption from Pt(111), Pt(533), Pt(755), and Pt(977)

Fig. 2 shows the H_2O desorption spectra from the four surfaces as well as the deconvolution into two or three Gaussian line shapes. Although the fits are not perfect, they give a good approximation for the integrated peak areas. On Pt(111) (Fig. 2a), the water desorption spectrum shows two peaks located at 168 K and 152 K. For low water dosage, only the high temperature peak is observed and it shifts from around 163 K to 168 K with increasing water coverage. These results are very similar to the results that Daschbach *et al.* reported for

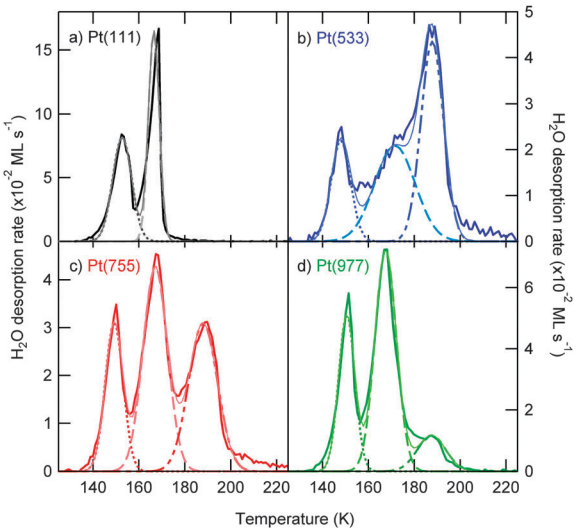

Fig. 2 Deconvolution of the H_2O desorption spectra from bare surfaces into (a) two Gaussians for Pt(111), and into three Gaussians for (b) Pt(533), (c) Pt(755), and (d) Pt(977).

sub-monolayer water desorption from Pt(111).[19] They used a heating rate of 0.6 K s^{-1} and dosed water at 100 K. Their water desorption peak shifts from ~158 K for very low water coverage to ~168 K for 1 ML of water. When more than 1 ML of water is dosed, a second lower-temperature peak appears that shifts from approximately 148 K to 158 K with increasing water coverage (not shown). Since Daschbach *et al.* did not report a second peak, we compare these results to results from Haq *et al.*[17] They dosed water at a slightly higher temperature of 137 K, in order to obtain a CI film on the Pt(111) surface, and used a heating rate of 0.65 K s^{-1}. They also observed a peak shifting from ~160 K to 168 K with increasing water dosage corresponding to submonolayer water desorption from Pt(111). In their work, with more than 1 ML dosed onto the surface, a low temperature peak appears that shifts from ~148 K to 152 K for 1.7 ML of water. This low temperature peak was assigned to water desorption from the second layer. Since our results are very similar to these literature results, we also assign the high temperature peak (around 168 K) to water desorption from the bare Pt(111) and the low temperature peak (around 152 K) to water desorption from water in the second layer.

For Pt(533) (Fig. 2b), the water desorption spectrum is deconvoluted into three Gaussian line shapes. We have reported the results of water desorption from bare Pt(533) in an earlier publication[43] and for completeness' sake we summarize the main findings here briefly. For water coverages below 0.25 ML, there is a peak around 184 K that shifts to 188 K with increasing coverage. For coverages higher than 0.25 ML, this peak does not shift anymore until saturation of this peak. A second intermediate temperature peak (around 167 K) appears prior to saturation of the high temperature peak. When both the high and intermediate temperature peaks are saturated, a third low temperature peak appears around 150 K shifting to higher temperatures with increasing water dosage. We assigned the peak at 188 K to water desorption from the (100) steps on the Pt(533) surface, the peak at 167 K to water desorption from (111) terrace sites on this surface, and the peak around 150 K to desorption from the second water layer. The water desorption spectra from both Pt(755) (Fig. 2c) and Pt(977) (Fig. 2d) also show three peaks, located at 188 K, 167 K, and around 150 K. Fig. 3b collects the TPD spectra in one figure and clearly shows that the desorption peak of water in the second layer, the desorption peak of water from (111) terraces, and the desorption peak of water from the (100) steps show perfect correspondence for all three stepped surfaces. The two low temperature peaks of the stepped surfaces also align with the peaks from Pt(111) corresponding to water desorption from the monolayer and second layer. The amount of water desorption from steps decreases with decreasing step density from Pt(533) to Pt(755) to Pt(977) and eventually disappears for Pt(111), whereas the amount of water desorption from (111) sites increases. Since the peak temperatures of the spectra of Pt(755) and Pt(977) are very similar to those of Pt(533) (and Pt(111)), we assign the low temperature peaks (around 150 K) in Fig. 2c (Pt(755)) and Fig. 2d (Pt(977)) to desorption of water in the second layer, the peaks at 167 K to water desorption from the (111) terraces, and the peaks at 188 K to water desorption from the (100) steps on Pt(755) and Pt(977).

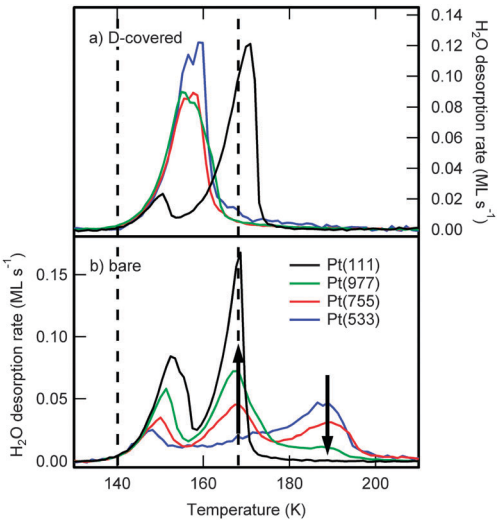

Fig. 3 Comparison of H_2O TPD spectra from (a) D-covered, and (b) bare Pt(111) (black), Pt(533) (blue), Pt(755) (red), and Pt(977) (green).

Table 1 Terrace width, step density, water desorption from steps to terrace ratio, and peak width FWHM for Pt(111), Pt(977), Pt(755), and Pt(533)

Surface	Terrace width	Step density ($Å^{-1}$)	INT(step)/ INT(ter)	Terrace peak FWHM (K)	Step peak FWHM (K)
Pt(111)	Infinity	—	—	5.6	—
Pt(977)	8	0.054	0.21	11.2	14.6
Pt(755)	6	0.072	0.86	12.6	14.9
Pt(533)	4	0.109	1.16	20.8	11.6

It is informative to analyze the Gaussian line shapes for the water desorption peaks from (111) terraces and from (100) steps (Fig. 2). Table 1 compares the ratio between the integral of the (100) step site peaks to the (111) terrace site peaks to the step density for the three stepped Pt surfaces. Pt(533) has a step density of 0.109 $Å^{-1}$. For instance, the ratio between the step peak and the terrace peak is 1.16 for this surface. Even though we describe Pt(533) as a surface of 4 atom wide (111) terraces, separated by (100) steps, the presence of steps seems to have a larger influence on the stabilization of water as would be expected from pure geometrical considerations. DFT (density functional theory)[38] and STM[21] studies have suggested that water molecules desorbing in the high temperature peak, may originate from both the upper and lower sides of the (100) steps and maybe also at least in part from the (111) terraces close to the steps. For Pt(755), with a step density of 0.072 $Å^{-1}$, the ratio between step stabilized water and terrace stabilized water is 0.86, and for Pt(977), with a step density of 0.054 $Å^{-1}$, this ratio is 0.21. The relative amounts of step- *vs.* terrace-bound water exhibit non-intuitive and non-linear changes with step density and terrace width. The ratio between the step stabilized water *vs.* the terrace stabilized water decreases faster with increasing terrace width than expected from the geometry of the surfaces. This indicates that the binding of water near steps seems to influence water at terraces more when the terraces are shorter.

It appears that this is mirrored by the width of the intermediate temperature peak corresponding to water desorbing from (111) terraces. On Pt(111), this peak is rather sharp with a full width at half maximum (FWHM) of 5.6 K. The peak becomes broader as the terrace width decreases from 8 atom wide terraces (FWHM of 11.2 K for Pt(977)) to 6 atom wide terraces (FWHM of 12.6 K for Pt(755)) to 4 atom wide terraces (FWHM of 20.8 K for Pt(533)). At the same time, the (100) step peak width increases from 11.6 K on Pt(533) to 14.9 K on Pt(755). The peak of water desorption from the (100) steps on the Pt(977) surface is relatively small, which causes the slightly more narrow peak width (14.6 K) compared to the step peak width of the Pt(755) surface. Nevertheless, the variation in the peak width corresponding to water desorption from steps appears less than in the peak width variation for water desorbing from the terraces. The sharpness of the TPD peak is a measure of the lateral interactions between the species desorbing in the peak, a narrower peak signifying more strongly attractive interactions.[44] On a Pt(111) surface, water forms a highly ordered 2-D network characterized by strong hydrogen bonding interactions. Introducing steps into the surface, breaks this 2-D order, weakening the overall influence of lateral hydrogen bonding. On a relatively narrow terrace such as on Pt(533), this much reduced 2-D hydrogen bonding network leads to a broad peak. The more moderate variation in peak width from step desorption suggests a more 1-D type nature of the lateral interactions on the steps. This interpretation in consistent with STM imaging of low water coverages on Pt(111), where H_2O binds initially along step edges only.[21]

Summarizing, steps influence the binding of water to well-defined platinum surfaces in a way that is long-ranged and that cannot be considered as an additive perturbation to the terrace adsorption of water. Steps break the ability of terrace-bound water to hydrogen bond, and the number of water molecules whose binding energy is influenced by the presence of steps is a non-linear function of step density.

3.2 H_2O desorption from D pre-covered Pt(111), Pt(533), Pt(755), and Pt(977)

Fig. 3 shows a comparison between water TPD spectra from (a) completely D-precovered and from (b) bare Pt(111), Pt(533), Pt(755), and Pt(977). Pt(111) shows two water desorption peaks for both the bare surface and the D-precovered surface. The low temperature peak depends on the amount of water in the second layer that is dosed on the (D-precovered) surface and will therefore not be discussed in detail. The high temperature peak is located at a slightly higher temperature for the completely D-precovered Pt(111) surface (171 K) compared to the bare Pt(111) surface (168 K). This stabilization of water on D-precovered Pt(111) has been noted before by Petrik and Kimmel,[40] who observed a high temperature peak for D_2O desorption located at 170 K. For small amounts of predosed deuterium, their peak was stabilized up to a temperature of 175 K. When more deuterium precovers the surface, this stabilization decreased to a peak temperature of 171 K for the completely D-precovered Pt(111) surface. Note that this

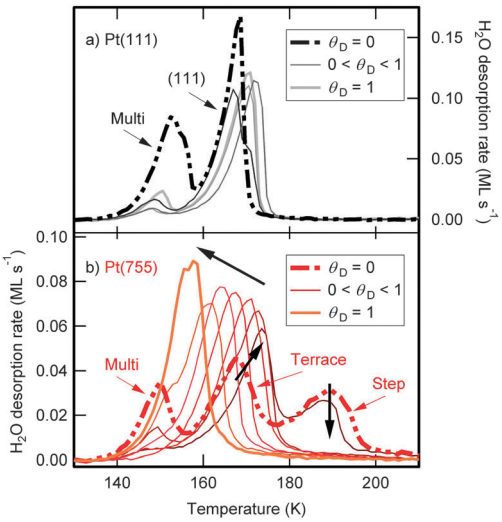

Fig. 4 H_2O TPD spectra for various pre-coverages of D on (a) Pt(111), and (b) Pt(755). Consecutive D-coverages for Pt(111) are 0, 0.20, 0.47, 0.97, and 1.0 ML. Consecutive D-coverages for Pt(755) are 0, 0.06, 0.17, 0.33, 0.54, 0.71, 0.84, and 1.0 ML.

desorption temperature indicates that water is still more stable on the completely D-precovered surface than on the bare Pt(111) surface. Our water desorption peak temperatures are somewhat different compared to those of Petrik and Kimmel, but the trends are the same. Our bare Pt(111) surface shows a water desorption temperature of 168 K. When half of this surface is precovered with D (Fig. 4a), the desorption temperature increases to 172 K. When the surface is completely precovered with D, the temperature decreases to 171 K, but it is still more stable than on bare Pt(111). Apparently water can still form a stable 2D hydrogen-bonded network on the D/Pt(111) surface and it is slightly more stable than on the bare Pt(111) surface.

Whereas water desorption from bare Pt surfaces with (100) steps show three peaks for the water desorption, *i.e.* at 188 K (steps), 167 K (terraces), and around 150 K (second and multilayer), the completely D-precovered surfaces only exhibit one peak corresponding to the multilayer water desorption regime for all three stepped surfaces. Even Pt(977), with eight atom wide (111) terraces, shows only a single desorption feature for water when the surface is completely precovered with D. The water destabilization on D/Pt(533) has been described in an earlier publication[43] and has also been compared to D/Pt(553).[41] Close to deuterium saturation of the Pt(533) surface, water forms 3-D ASW clusters near step sites. These ASW clusters are large enough to show a deflection in the TPD spectra at a temperature of around 157 K, which is characteristic of ASW transformation into CI.[43,45] This implies that H_2O no longer spreads over the surface to form a hexagonal structure with hydrogen bonds, suggesting the hydrophobic character of D/Pt(533). The step-bound D also disrupts the tendency of water to organize itself neatly in 1-D chains along the upper edge of the (100) step. Initial adsorption of H_2O forms D–H_2O clusters, which can be subsequently hydrated by additional H_2O. Broadening the 4 atom wide

(111) terraces of Pt(533) to the 6 or 8 atom wide (111) terraces of Pt(755) and Pt(977), still results in a completely hydrophobic surface when fully precovered with D. These surfaces exhibit a single water desorption peak in the second water layer desorption regime, with the deflection of ASW crystallization into CI around 157 K. Since D/Pt(111) and D/Pt(977) show very different water adsorption properties, it seems that the (100) steps have a very strong and long-ranged influence on the surface hydrophobicity, particularly when the surface is precovered with D. On the bare surfaces, the influence of the (100) steps is less pronounced for broader terraces (Fig. 2 and 3b), with the broadness of the peak suggesting that water forms a more extensive hydrogen bonded network on the broader (111) terraces. However, on the D-precovered surfaces with (100) steps, the terrace width has essentially no impact on the water desorption, at least not for the terrace widths considered here. Apparently the step-bound D forces water to form 3-D ASW clusters near step sites largely independent of the width of the neighboring terraces. The stable water layer that adsorbs on the D-covered Pt(111) surface is completely absent on the stepped surfaces, even on Pt(977). This illustrates the highly long-ranged effect that steps may exert on water adsorption, even on well-ordered Pt surfaces.

To illustrate the role of the coverage by D, Fig. 4 compiles water desorption spectra from Pt(111) (a) and Pt(755) (b) for various amounts of D pre-coverage. When D pre-covers a Pt(111) surface, the H_2O monolayer is first stabilized, but for higher D-precoverage the temperature shifts back to a temperature that is just slightly higher than water desorption from the bare surface, as was discussed above. For the stepped Pt(533) (not shown), Pt(755), and Pt(977) (not shown) surfaces, the H_2O stabilization near (100) step sites rapidly disappears when small amounts of deuterium precover the step sites. The water desorption from (111) terraces is only observed for small amounts of D-precoverage on all stepped surfaces. As on Pt(111), this desorption temperature increases first when a small amount of D is present. In contrast to Pt(111), increasing the D coverage on the stepped surfaces destabilizes water adsorption on the (111) terraces very rapidly, until the surfaces become completely hydrophobic as manifested by water adsorbing as ASW near step sites.

Fig. 5a plots the shift in maximum desorption temperature for water desorption from the (111) facets (the peak around 167 K) of Pt(111), Pt(533), Pt(755), and Pt(977) as a function of the deuterium coverage on the step sites (θ_D step) and on the terrace sites (θ_D terrace). There are three different influences of the D coverage. First, when D is precovering the (100) step sites, H_2O stabilization near step sites (the peak around 188 K) rapidly disappears. The second effect is that water on the (111) terraces (the peak around 167 K) is stabilized when D is precovering the step sites, which was also observed on Pt(111), where the desorption temperature increases first when a small amount of D is precovering the surface. On all stepped surfaces, the desorption temperature of the H_2O peak has a maximum when the steps are precovered with D. The third influence of D is that when D starts to precover the (111) terrace sites, on the stepped surfaces this leads to a destabilization of water on the

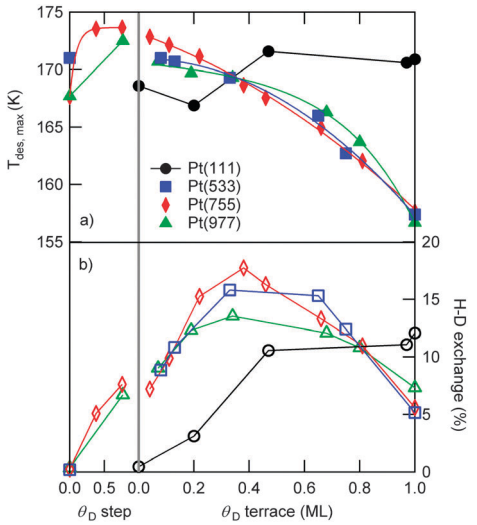

Fig. 5 (a) Maximum desorption temperature, and (b) the percentage of H–D exchange, as a function of D coverage on the (100) steps and (111) terraces for Pt(111) (black circles), Pt(533) (blue squares), Pt(755) (red diamonds), and Pt(977) (green triangles). Lines are only a guide for the eye.

(111) terraces. The desorption temperature drops to the value where the second water layer desorption takes place. This means that all stepped surfaces become hydrophobic when the whole surface is precovered with D, whereas on D pre-covered Pt(111), the water is stabilized, as clearly illustrated in Fig. 5a.

Fig. 5b shows the percentage of H–D exchange between H_2O and deuterium as a function of θ_D step and θ_D terrace. This percentage is determined by taking the integral of the HOD (one H–D exchange) and two times the D_2O (two H–D exchanges) signal divided by the integral of the total water desorption (combined H_2O, HOD, and D_2O signal). All three stepped surfaces show a maximum H–D exchange when approximately 0.4 ML of deuterium precovers the terraces. This does not appear to depend on the actual terrace width, but only on the percentage that is covering the terraces. Again, Pt(111) shows completely different behavior. For this surface, the amount of exchange always increases with increasing D coverage. It seems that the (100) steps catalyze the exchange reaction between H and D atoms from H_2O and D_2, since the amount of exchange on all stepped surfaces is higher than on the Pt(111) surface. However, for a D-precoverage higher than around 0.4 ML, the amount of exchange on the stepped surfaces starts to decrease. When more than around 0.8 ML of D is precovering the stepped surfaces, the total amount of H–D exchange is smaller than the H–D exchange on Pt(111). This is in agreement with the idea that when the (111) terraces of the stepped surfaces are precovered with D, the stepped surface becomes hydrophobic, forcing water into ASW snowballs on the steps. As a result, a smaller fraction of the adsorbed water is in direct contact with D/Pt(S), resulting in a lower H–D exchange. We believe that the exchange between D and H_2O takes place through the formation of a hydronium intermediate, which have been observed on Pt(111)[46] and Pt(100)[47] by infrared spectroscopy.

4 Conclusion

In this paper, we have shown that truncating an infinite (111)-type terrace by the introduction of steps, may affect the surface chemistry and surface physics of water in a way that does not scale linearly with terrace width or step density. Strong lateral interactions and step-induced preferences in adsorption or orientation affect binding of water at terrace sites even if they seem significantly remote from the step edge. Introduction of steps significantly perturbs the energetics of water ordering on (111) terraces, as evidenced by broadening of the water desorption peak from (111) terraces. Interestingly, the width of the peak corresponding to water desorption from steps is much less influenced by terrace width, testifying to the 1-D character of water interactions at steps. In the presence of D on the stepped Pt surfaces with (100) steps, a high D coverage makes all water accumulate at the step sites, largely independent of terrace width. These remarkable observations illustrate the highly subtle interactions between H_2O, D and Pt, showing that a stepped or defected surface in contact with water is far from a linear combination of terrace and step/defect effects. Steps exert a long-ranged effect on the adsorption of water on well-defined platinum surfaces; in the presence of hydrogen or deuterium, this even leads to an adsorption behavior that is completely dominated by steps, even for relatively wide terraces. We believe that these results may have important implications for catalytic reactions taking place at the platinum–water interface, as we expect that the fundamental interactions responsible for this behavior will still be present at higher pressures and temperature.

Acknowledgements

This work was supported financially by the National Research School Combination Catalysis (NRSC-C) and the Netherlands Organization for Scientific Research (NWO).

References

1 D. Chandler, *Nature*, 2005, **437**, 640–647.
2 R. Baldwin, *Science*, 2002, **295**, 1657–1658.
3 K. A. Dill and J. L. MacCallum, *Science*, 2012, **338**, 1042–1046.
4 N. Levinger, *Science*, 2002, **298**, 1722–1723.
5 M. Wong, J. Thomas and T. Nowak, *J. Am. Chem. Soc.*, 1977, **99**, 4730–4736.
6 M. R. Hogerheijde, E. A. Bergin, C. Brinch, L. I. Cleeves, J. K. J. Fogel, G. A. Blake, C. Dominik, D. C. Lis, G. Melnick, D. Neufeld, O. Panic, J. C. Pearson, L. Kristensen, U. A. Yildiz and E. F. van Dishoeck, *Science*, 2011, **334**, 338–340.
7 B. Nisini, *Science*, 2000, **290**, 1513–1514.
8 S. Ioppolo, H. M. Cuppen, C. Romanzin, E. F. van Dishoeck and H. Linnartz, *Astrophys. J.*, 2008, **686**, 1474–1479.
9 F. Schreiber, *J. Phys.: Condens. Matter*, 2004, **16**, R881–R900.
10 D. Schwendel, T. Hayashi, R. Dahint, A. Pertsin, M. Grunze, R. Steitz and F. Schreiber, *Langmuir*, 2003, **19**, 2284–2293.
11 G. Hummer, J. Rasaiah and J. Noworyta, *Nature*, 2001, **414**, 188–190.
12 S. Granick and S. C. Bae, *Science*, 2008, **322**, 1477–1478.
13 H.-J. Wang, X.-K. Xi, A. Kleinhammes and Y. Wu, *Science*, 2008, **322**, 80–83.
14 P. A. Thiel and T. E. Madey, *Surf. Sci. Rep.*, 1987, **7**, 211–385.
15 M. A. Henderson, *Surf. Sci. Rep.*, 2002, **46**, 1–308.
16 A. Hodgson and S. Haq, *Surf. Sci. Rep.*, 2009, **64**, 381–451.
17 S. Haq, J. Harnett and A. Hodgson, *Surf. Sci.*, 2002, **505**, 171–182.
18 J. Carrasco, A. Michaelides, M. Forster, S. Haq, R. Raval and A. Hodgson, *Nat. Mater.*, 2009, **8**, 427–431.
19 J. L. Daschbach, B. M. Peden, R. S. Smith and B. D. Kay, *J. Chem. Phys.*, 2004, **120**, 1516–1523.
20 K. Thürmer and S. Nie, *Proc. Natl. Acad. Sci. U. S. A.*, 2013, **110**, 11757–11762.
21 M. Morgenstern, T. Michely and G. Comsa, *Phys. Rev. Lett.*, 1996, **77**, 703–706.
22 K. Morgenstern, *Surf. Sci.*, 2002, **504**, 293–300.
23 M. T. M. Koper, *Nanoscale*, 2011, **3**, 2054–2073.
24 J. Blackman, *Metallic Nanoparticles*, Handbook of Metal Physics, Elsevier, 2009.
25 G. B. Fisher and J. L. Gland, *Surf. Sci.*, 1980, **94**, 446–455.
26 B. A. Sexton, *Surf. Sci.*, 1980, **94**, 435–445.
27 E. Langenbach, A. Spitzer and H. Lüth, *Surf. Sci.*, 1984, **147**, 179–190.
28 U. Starke, K. Heinz, N. Materer, A. Wander, M. Michl, R. Döll, M. A. van Hove and G. A. Somorjai, *J. Vac. Sci. Technol., A*, 1992, **10**, 2521–2528.
29 X. Su, L. Lianos, Y. R. Shen and G. A. Somorjai, *Phys. Rev. Lett.*, 1998, **80**, 1533–1536.
30 A. L. Glebov, A. P. Graham and A. Menzel, *Surf. Sci.*, 1999, **427–428**, 22–26.
31 M. Nakamura, Y. Shingaya and M. Ito, *Chem. Phys. Lett.*, 1999, **309**, 123–128.
32 H. Ogasawara, J. Yoshinobu and M. Kawai, *J. Chem. Phys.*, 1999, **111**, 7003–7009.
33 K. Jacobi, K. Bedürftig, Y. Wang and G. Ertl, *Surf. Sci.*, 2001, **472**, 9–20.
34 G. Zimbitas and A. Hodgson, *Chem. Phys. Lett.*, 2006, **417**, 1–5.
35 G. Zimbitas, S. Haq and A. Hodgson, *J. Chem. Phys.*, 2005, **123**, 174701.
36 G. A. Kimmel, N. G. Petrik, Z. Dohnálek and B. D. Kay, *J. Chem. Phys.*, 2006, **125**, 044713.
37 D. C. Skelton, R. G. Tobin, G. B. Fisher, D. K. Lambert and C. L. DiMaggio, *J. Phys. Chem. B*, 2000, **104**, 548–553.
38 M. L. Grecea, E. H. G. Backus, B. Riedmüller, A. Eichler, A. W. Kleyn and M. Bonn, *J. Phys. Chem. B*, 2004, **108**, 12575–12582.
39 M. J. T. C. van der Niet, A. den Dunnen, L. B. F. Juurlink and M. T. M. Koper, *J. Chem. Phys.*, 2010, **132**, 174705.
40 N. G. Petrik and G. A. Kimmel, *J. Chem. Phys.*, 2004, **121**, 3727–3735.

41 M. J. T. C. van der Niet, A. den Dunnen, M. T. M. Koper and L. B. F. Juurlink, *Phys. Rev. Lett.*, 2011, **107**, 146103.
42 A. den Dunnen, M. J. T. C. van der Niet, M. T. M. Koper and L. B. F. Juurlink, *J. Phys. Chem. C*, 2012, **116**, 18706–18712.
43 M. J. T. C. van der Niet, I. Dominicus, M. T. M. Koper and L. B. F. Juurlink, *Phys. Chem. Chem. Phys.*, 2008, **10**, 7169–7179.
44 A. Cordoba and J. J. Luque, *Phys. Rev. B: Condens. Matter Mater. Phys.*, 1982, **26**, 4028–4034.
45 P. Lofgren, P. Ahlstrom, D. Chakarov, J. Lausmaa and B. Kasemo, *Surf. Sci.*, 1996, **367**, L19–L25.
46 D. Lackey, J. Schott, J. K. Sass, S. I. Woo and F. T. Wagner, *Chem. Phys. Lett.*, 1991, **184**, 277–281.
47 N. Kizhakevariam and E. M. Stuve, *Surf. Sci.*, 1992, **275**, 223–236.